Published in final edited form as:
Adv Funct Mater. 2011 July 22; 21(14): 2624–2632. doi:10.1002/adfm.201002429.

Biohybrid Carbon Nanotube/Agarose Fibers for Neural Tissue Engineering

Dan Y. Lewitus[**],
The New Jersey Center for Biomaterials, and Department of Biomedical Engineering Rutgers, the State University of New Jersey, 145 Bevier rd. Piscataway, NJ, 08854 (USA)

John Landers[**],
Department of Chemical and Biochemical Engineering, Rutgers, State University of New Jersey, Piscataway, NJ, 08854, USA

Jonathan Branch,
The New Jersey Center for Biomaterials, and Department of Biomedical Engineering Rutgers, the State University of New Jersey, 145 Bevier rd. Piscataway, NJ, 08854 (USA)

Karen L. Smith,
Wadsworth Center, New York State Department of Health, 1 Government Center, Albany NY, 12201 (USA)

Gerardo Callegari,
The Center for Modeling and Characterization of Nanoporous Materials, TRI/Princeton, Princeton, NJ 08542 USA

Joachim Kohn, and
The New Jersey Center for Biomaterials, and Department of Biomedical Engineering Rutgers, the State University of New Jersey, 145 Bevier rd. Piscataway, NJ, 08854 (USA)

Alexander V. Neimark
Department of Chemical and Biochemical Engineering, Rutgers, State University of New Jersey, Piscataway, NJ, 08854, USA

Joachim Kohn: kohn@rutgers.edu; Alexander V. Neimark: aneimark@rutgers.edu

Abstract

We report a novel approach for producing carbon nanotube fibers (CNF) composed with the polysaccharide agarose. Current attempts to make CNF's require the use of a polymer or precipitating agent in the coagulating bath that may have negative effects in biomedical applications. We show that by taking advantage of the gelation properties of agarose one can substitute the bath with distilled water or ethanol and hence reduce the complexity associated with alternating the bath components or the use of organic solvents. We also demonstrate that these CNF can be chemically functionalized to express biological moieties through available free hydroxyl groups in agarose. We corroborate that agarose CNF are not only conductive and nontoxic, but their functionalization can facilitate cell attachment and response both *in vitro* and *in vivo*. Our findings suggest that agarose/CNT hybrid materials are excellent candidates for applications involving neural tissue engineering and biointerfacing with the nervous system.

Correspondence to: Joachim Kohn, kohn@rutgers.edu; Alexander V. Neimark, aneimark@rutgers.edu.
[**]These authors equally contributed to this manuscript

Supplementary Information
Supporting Information is available online from Wiley InterScience or from the author.

Keywords

Carbon-nanotubes; agarose; fibers; functionalization; neural

1. Introduction

It is generally recognized that cortical neural prosthetic devices are limited to 12 months or less before their recording performance deteriorates substantially.[1, 2] This limitation lies with the fact that a sustained reactive response develops upon insertion of the probe. This response, known as gliosis, diminishes the long-term performance of devices.[1, 3–5] ontrol of the brain cell response to the inserted device could lead to improvement of its long-term performance. A number of approaches have been considered, both in terms of biochemistry and design. Examples include the addition of anti-inflammatory agents[5–9] or cell cycle-inhibiting drugs,[9, 10] as well as surface modification of silicon substrates.[9, 11–13] Nevertheless, these approaches are burdened by the large stiff constructs that will be present in the tissue throughout its lifetime. To circumvent this, an approach has recently emerged relying on two principals. First, these devices should be made of flexible materials. This will reduce the mechanical disparity between the device and the brain and possibly reduce development of the chronic glial response,[9, 14–18] Second, devices smaller in size, comparable to the neuronal soma, could lead to a reduction in the chronic glial response through the restoration of neuronal and astroglial synapses.[17, 19, 20] Therefore, smaller and more flexible devices may reduce reactive responses and improve long-term performance, e.g. recording of neural signals.

In this work, a new material comprised of carbon nanotubes (CNT) and the polysaccharide agarose, which is promising for fabrication of neural probes that may reduce the limitations stated above. CNT display unique characteristics of superior conductivity, tremendous stiffness and a high aspect ratio. As such, they have been extensively employed in novel materials[21–23] stemming from their ability to absorb strain and induce conductivity. In addition, it has been shown that macroscopic materials made out of CNT are in fact biocompatible,[24, 25] making their inclusion into materials destined for medical applications that much more promising. Indeed, this coincides with reports that the incorporation of carbon nanotubes maintains a material's structural stability during cell growth.[26] This attribute is coupled with the fact that CNT can support neuron cell growth and differentiation,[24, 27] a decisive factor for any device that hopes to induce electrical stimulation with neurons in vivo. The evolving interest in natural polymers destined for drug delivery and tissue engineering has led to the emergence of new hybrid materials. So far a popular method to fabricate CNT/polymer hybrids is through the technique of wet spinning.[23, 24, 28–34] Wet spinning has been utilized in producing CNT/polymer composite fibers for the last 10 years.[21, 23, 30] Despite its inherent advantage, the ability to scale up the production of CNT fibers, specifically those intended for biomedical applications, incurrs some drawbacks. This concept has been previously invoked where a polymer, such as PVA, is utilized as either the bath component or the dispersant. The former leads to several shortcomings which make the process difficult to scale commercially. The primary concern arises when the gel ribbon becomes suspended at the spinning position. Thus it is necessary to continually raise the tip of the spinning bath to prevent the ribbon from clashing into itself. However, with the removal of the polymer from the bath there is a reduction in several degrees of freedom inherent to how the polymer solution is prepared. Several authors have demonstrated this practicality by using the polymer as the dispersant.[28, 30, 31, 34] This provides several technical advantages, including the fact that the spun ribbon can be reeled up onto a spool. Alterative methods have been proposed, which lead to a cleaner product and less expensive process.[30] The use of polymeric

hydrogels has a certain advantage due in part to their ability to imitate the natural extra cellular matrix (ECM), thus promoting cell growth.[33, 35] Lastly, deciphering the composition of the fiber becomes easier as it is dependent only on the initial concentrations of the dispersion. This is contrary to analyzing the fiber *post facto* when it is spun into a polymer bath which will be dependent on the polymer concentration and adsorption kinetics.

In this process, CNT are dispersed with the aid of a surfactant or polymer by non-covalent means. The literature is scattered with examples of polymers which aid in this process.[32, 34] Some of these materials are based on the use of natural polymers or naturally based dispersant that are known to be biocompatible, such as chitosan, hyaluronic acid, DNA and chondroitin sulfate.[29, 31] However, both chitosan and hyaluronic acid are biodegradable and are undesirable for long-term indwelling recording electrodes. One alternative which is absent from the current list of proposed polymers is the naturally occurring polysaccharide agarose.

Agarose is an algae derived linear polysaccharide hydrogel possessing a sub-micron pore structure. It is a poly(1→4)-3,6-anhydro-α-l-galactopyranosyl-(1→3)-β-d-galactopyranose) with thermoreversive properties. Although it is a non cell adherent, due to its benign and biocompatible nature, it is commonly used as a non adhesive substrate for in vitro cell studies.[36] In addition, agarose has several distinct advantages over other natural polymers: (A) its thermal dependant hydrogel properties allow it to be easily malleable into different shapes and forms without the use of additional reagents or organic solvents. (B) Unlike extracellular matrix based polymers, specific proteins or DNA, it lacks native ligands and is thus inert to mammalian cells.[37] (C) Through available primary and secondary hydroxyl groups, agarose can be chemically modified. This leads to a functionalization through grafting of proteins, peptides and glycogens to the polysaccharide backbone, allowing it to be specifically tailored for various biorelevant applications.[38–40] (D) The addition of such molecules can alter not only its biocompatible properties, but its mechanical properties as well. (E) Its high surface to volume ratio and porosity[37, 41] combined with its hydrophilic nature allows for a more effective penetration of cells during seeding while supporting delivery of nutrients and metabolites to these cells.[38, 39] Carrying out such modifications will result in a substantial increase in cell attachment, continuous support of 3D neural cell cultures, the ability to orient cell migration, and specifically enhance neurite extension with the grafting of neuron conductive constituents such as laminin or various oligopeptides.[38, 39] (F) Unlike other biopolymers, it is non-biodegradable, therefore will allow for long term performance and integration of the carbon nanotubes and avoid disintegration of the fabricated structures.[37] (G) Agarose is a cheap and abundant polysaccharide, sourced from plants (algae) and can be grown in highly controlled environments. This is compared with the prohibitive cost associated with making fibers with either DNA or hyaluronic acid. Due to these reasons, agarose has found use in the field of neural engineering and nerve regeneration where it has been suggested as the primary support construct in nerve guide conduits.[37, 42]

In this work, we aim to combine three elements that have not yet been adjoined, the ease of wet spinning as a fabrication technique, with the reinforcing and conductance properties of CNT's, along with the gelation and functionalization potential of agarose, to create a continuous, electro and neuron conductive biohybrid nanocomposite fiber. The consequence of which is a fiber that is stiff when dry yet flexible when hydrated. We believe the impact of this work will provide a foundation for long-term neural recording devices as an alternative to silicone/metal based electrodes in the quest to evade gliosis and performance degradation.

2. Results and Discussion

2.1. Fiber Fabrication

Fibers were fabricated by two methods, wet spinning and molding the fiber in a hollow tube. In the former the liquid dispersion used to make the fibers was injected into a rotating bath, with the rotation velocity larger than the injecting velocity. Upon entering the bath, the dispersion displays an axial diffusion which is inhibited by two factors. First, the stretching imposed by the rotating velocity field and second by the gelation of the agarose/CNT composite. By controlling the speed and the rheology of the injecting dispersion and the rotating solution, the width and morphology of the fiber precursor can be controlled. Therefore, a greater rotation speed may result in better alignment of the single walled carbon nanotubes (SWNTs) encapsulated in the agarose gel matrix.

SEM images of molded fibers are presented in Figure 1 a, b and c. This fabrication technique results in a smooth and nearly flat morphology. However, fibers fabricated by the wet spinning method (Figure 1 d, e and f) resulted in round circular fibers with a rough outer surface. This is the result of the extraction process from the bath where capillary forces fold the fiber precursor.[43] This ability to control the surface roughness has been determined to be a key parameter that affects the quality of cellular interfacing between CNT's and cultured neurons.[44] For both types of fibers, a close inspection of the cross section will show the exposure of carbon nanotube bundles depicted in Figure 1 c and f evident by the long overlapping strands. A degree of alignment, which is critical to improvements in mechanical and electrical properties[45], is still obtained when molding is used. This is most likely induced when the dispersion is first injected into the tube. The TEM images shown in Figure 2 support this assumption, where longitudinal cross sections of CNT fibers demonstrate general orientation in the direction of the fiber.

2.2. Agarose Fiber Functionalization

Functionalized and control fibers were qualitatively evaluated by both fluorescent microscopy and fluorescent intensity reading. Representative fluorescent and phase contrast images of functionalized ("protein"+) and control fibers ("protein"−) are shown in Figure 3. Fluorescein conjugated bovine serum albumin (BSAC) allows for direct attachment verification. Since the protein has a fluorescent marker conjugated, its covalent attachment will result in fibers with inherent fluorescence. Indeed functionalized fibers demonstrate high fluorescence, compared to the control fiber (Figures 3a & 3b). The validation of laminin attachment to the agarose carbon nanotube fibers was performed using an immunohistochemical (IHC) technique as shown in Figure 3c. This method allowed not only validation of the attachment, but also to some extent confirmed the retention of the protein conformation, as the primary antibody used is specific for laminin. Moreover, the immunofluorescence of the fibers reveals that the agarose orientates itself longitudinally with the fiber. This feature is most likely due to the elongation of the dispersion when it experiences the rotating velocity field during the fabrication process. Fibers placed in a black 96 well plate were tested for fluorescence intensity using a plate reader. Results for LN and BSAC functionalized fibers and their prospective controls are shown in Figure 3d and Figure 3e respectively. The control and pristine fibers exhibited low values of fluorescence intensity (FI) with no statistical difference between them ($P>0.05$). The functionalized fibers FI values were 2 orders of magnitude higher than those of the other two types ($P<0.05$), indicating successful functionalization. The actual quantification of the functionalized sites by the CDAP chemical reaction and amount of bound proteins was not performed, though could be possible based on the barbituric acid assay.[40] These findings emphasize the advantage of using agarose. It is a "clean slate" for biochemcal manipulation. This allows for specific cellular cues and even several different cues to be covalently

conjugated to the fibers, resulting in functionalized material thus allowing for specific use and application.

2.3. Mechanical Properties

The results of the mechanical tensile testing are shown in Table 1. Fiber stability was evaluated through hydration at a temperature close to the agarose mp (50 °C). The dry fibers exhibited stiffness close to over 1 GPa, with the pristine fibers being the stiffest. All fibers exhibited a rigid and tough behavior, with none of them failing through a brittle manner, but rather maintaining their strength past the yield point until complete failure. Such intrinsic strength in the dry state surpasses the critical strength required for pial penetration, reported to be (0.3–1.3 MPa). Moreover, the low strain values allow for minimal collateral damage during insertion process[46]. Once hydrated, only the CDAP functionalized fibers (LN+ and CDAP+) exhibited enough mechanical integrity to be evaluated and studied for their tensile properties). A 90% and 80% drop in the elastic modulus for the LN+ and CDAP+ respectively was observed for hydrated fibers in, accompanied with a decrease in yield and maximal strain. These reduced strength values in the kPa range bring the fiber's properties closer (if still higher) to that of inherent brain tissue.[47]

When CDAP is added to the agarose, cyano-ester termini results, and is available to react with free amide groups in the reaction. Competing reaction exists, where either a carbamate or an imidocarbonate can be formed from the cyanate ester.[40] The latter forms either a cyclic bond within an agarose backbone or a crosslink between adjacent polymer chains, thus resulting in a slightly crosslinked and more stable CNT fiber (CDAP+). When laminin, a high molecular weight protein is added to the reaction (LN+), there is increased coupling, principally due to the available ε-amines of surface lysine. This in turn creates the formation of an isourea bond resulting in the observed CNF stability.[48] The late addition of the quenching ethanolamine to the functionalization reaction possibly leads to elevated density of the crosslinking imidocarbonate in the CDAP+ fibers. Moreover, we expect that the crosslinking density of the CDAP+ fibers would be higher than the LN+ samples since the distance between formed cross-linking junctions is shorter. We designed these fibers to be biological viable, conductive and supportive for soft tissue rather than applicable for load bearing applications. This plasticization process occurring due to water absorption brings the fiber's strength and modulus much closer to that of inherent brain tissue, thus become more compliant compared to silicon neural devices.[1] We do suspect that using a higher melting point agarose, with a higher molecular weight, could increase the strength of the composite fibers.[49] The chemical reaction itself through changes in reagent stoichiometry can be used to further modify the mechanical stability of the fibers in a biological environment.

2.4. Electrical properties

The results of the different fiber conductivities are presented in Table 2. The dual mechanical and conductive effect of having carbon nanotubes present in a material is essential for any composite. Electrical conductivity has been shown to support the growth of a variety of tissues such as cardiac muscle and neural tissue.[50] Furthermore, it is key for neurite extension, where electrical propagation assists in the growth of neurons on carbon nanotube deposited planar substrates.[51–53] The effect of which can be attributed to the carbon nanotubes acting as excellent free radical inhibitors.[54] This is due in part to their ability to either donate or accept electrons. As such, free radicals which are considered detrimental to cell viability, will be absent from the agarose fibers.

Dry samples of CNF prepared in this paper were shown to be electro-conductive with a specific conductivity of approximately (130–60 S cm^{-1}) (depending on the fiber batch). These values fall near the range of our previously reported results which used the polymer

PVA.[24] Likewise, these values are comparable with those for boron doped silicon, a material commonly used for fabrication of neural prosthetic devices.[55] In addition, we set out to test the fibers in buffer. The specific conductivity dramatically decreases in the pristine fiber when immersed in buffer (indeed almost 2 order of magnitudes), while the functionalized fibers show much less variation (LN+) and even no deterioration at all for the CDAP+ This implies that the cross-linking effect of the functionalization reaction impedes the swelling of the fiber, which then leads to a decrease in conductivity, possibly through disconnection of CNT bundles, affecting electrical paths.

2.5. Cytotoxicity and cell attachment

The metabolic activity of the cells exposed to different types of fibers was compared to positive-control cells kept in culture media. The effect of fiber presence on primary astrocyte culture viability is presented in Figure 4a. Tests revealed that the fibers had no effect on the cell viability ($p>0.05$). An exception would be the pristine fibers, where a slight (10%) statistically different reduction in viability was observed ($p<0.01$). This reduction is possibly due to presence of some catalyst residue in the CNT raw material. It is possible that the process of functionalization, involving multiple washing steps, redeemed the processed fibers from these toxic residues. It has also been reported that unpurified CNT containing a large amount of iron induces a inflammatory response in vivo by stimulating the production of reactive oxygen species (ROS).[56] When the CNT were purified to contain no impurities and subjected to a macrophage cell line, it was reported that no ROS production occurred.[57]

Cells attachment studies performed on molded composite discs revealed that only the LN functionalized composites, seen in Figures 4b and 4c, allowed for cell attachment while the control discs did not permit cell attachment. The agarose based materials maintain their biocompatibility properties, but are not permissive for cell attachment without the addition of cell adhesion moieties.[38, 39]

The process of conjugating peptides to the fabricated fibers was repeated several times successfully. It is a simple and safe process that does not require the use of a chemical hood or special safety measures.[40] Moreover, the cytotoxicity and cell attachment studies performed on primary brain cells prove the process to be non-toxic to mammalian cells.

2.6. *In Vivo* Evaluation

The insertion of fibers into a rat cerebral cortex was performed to allow preliminary evaluation of the insertion ability of the fibers into live tissue. This in turn permitted the acquisition of data with regard to the foreign body response inflicted by the presence of fibers in the tissue. Brain tissue inflammatory response to implanted materials is materialized through the presence of activated microglia and astrocytes at the vicinity of the implant site.[1, 58] Representative immunohistochemical images from sites where LN+ and LN− fibers were inserted into rat cortex are shown in Figure 5a and 5b. The intensities of astrocyte, microglia and neural expression measured for two of each fiber are shown in Figure 5c, 5d and 5e respectively.

The *in vivo* evaluation as to the effect of the inserted fibers on brain tissue reveals a slight effect to the functionalization with laminin on the formation of the glial response (gliosis). In both cases activation of microglia and astrocytes is observed corresponding to the formation of mild gliosis.[1, 58] The resulting extent of glia activation (approximately 100 μm of glial sheath formation) is similar in extent to data reported for other biocompatible materials such as silicon.[58] It has been reported that LN can reduce the extent of glial response when tethered to silicone devices and implanted for four weeks.[59] It is possible

that an extended period of implantation may have revealed a greater reduction in the response as a result of the presence of the laminin functionalized nanofibers.

Representative images of fibers extracted from brain tissue are shown in Figure 6. A difference between the fiber types could be observed once they were explanted. The laminin functionalized fibers seem to promote more cell adhesion compared to the non-functionalized ones. Laminin is an ECM protein that is known to enhance neural growth both *in vitro* and *in vivo*.[12, 59] Naturally, the attachment enhancement properties of such constituent will have effect on all cell types, as it is non-specific.[12] Finer manipulation of the foreign body response to the fibers can be achieved by the addition of more specific adhesion molecules to the fibers. Examples would be inflammatory response reducing agent such as alpha melanocyte stimulating hormone or neuron specific adhesion molecules such as L1 molecule. L1 has been shown not only to induce neurite outgrowth, but also to reduce astrocytic attachment. [12, 59, 60] Moreover, the explanted fibers demonstrated mechanical and dimensional stability. They became soft and pliable, in a trend similar to that shown with the mechanical tests.

In the central nervous system (CNS), such inherently conductive fibers could be developed into microscale neural recording devices. They can advance the field of neural prosthetics through long-term biocompatibility and performance by allowing the recording devices to interface with brain tissue. This in turn would allow for the enhancement of neural integration and the reduction of gliosis formation.[59] The materials characterized in this work could potentially function in the peripheral nervous system (PNS) as well. These fibers can be developed into intrafascicular electrodes, thus allowing for neural interfacing with the advantage of being both mechanically compliant and biologically attractive for long-term recording.[59] Additionally, in the PNS, nerve guidance conduits could be prepared either through molding of agarose/CNT dispersions,[42] or as fibers braided into nerve guide conduits. In the latter, their potential to support nerve growth and regeneration through electrical stimulation, porosity, and biochemical cues could prove advantageous.[61]

3. Conclusions

We have successfully fabricated agarose CNT hybrid fibers by taking advantage of agarose's ability to disperse and accommodate CNT's, its thermo responsive hydrogelation and its functionalization potential. These fibers are rigid and tough when dry, but exhibit mechanical properties compliant with brain tissue once hydrated. They prove to be not just non-toxic, but biocompatible, and biologically modifiable. These properties, along with their stable electrical conductance, provide a novel material with solid potential in future neurophysiologic applications. Although it was the scope of this paper to produce fibers for implantable electrodes, the gelling properties of agarose allows it to be easily molded into other shapes with alternative applications such as directed nerve repair and nerve guidance conduit.

4. Experimental

4.1 Fiber Fabrication

All chemicals were of reagent grade or higher. Fibers were produced from a dispersion containing 1 wt. % of SWNTs (Unidym or Nanoledge), 2 wt. % agarose (15517-014, Invitrogen,) and 97 wt. % distilled water. The dispersion was prepared with the aid of a horn sonicator (Mixsonix S400) for (10 min) at a pulsed rate of one second on and one second off. The sonicator was operated at (40 A). During the sonication process, enough heat is generated to invoke the transition of the agarose from an insoluble powder to a viscous liquid. This allows the agarose present in the liquid state to form random coils and

physically wrap around and disperse the SWNT without the use of additional dispersant such as a surfactant. While the dispersion is still a liquid, it is injected through a (1 mm) diameter tip into a bath of ethanol at room temperature rotating at a rate of 33 rpm, at which time it becomes a pre-fiber. The second approach produces (200 μm) fibers fabricated by injecting the dispersion into a 1 mm diameter tube and allowing it to gel. The subsequential molds are then flushed out with lukewarm water. Upon drying, these fibers shrink to ribbons (200 μm) wide. The characterization studies were performed mainly with the molded samples. Morphology of the fibers was evaluated using a Hitachi S-4500 Field emission SEM. Fresh cut sections were obtained by breaking the fibers after immersion for one min in liquid nitrogen. This process avoid smearing of the polymer/CNT nanostructures. The orientation of CNT in molded fibers was visualized using transmission electron microscopy. Fibers were embedded in embedding media (Electron Microscopy Sciences) and sectioned longitudinally with a diamond knife (Ultracut E ultramicrotome) at room temperature. Thin sections were applied on a copper Formavar / carbon coated grids (Electron Microscopy Sciences). Electron micrographs were taken using a model JEM 100 CX transmission electron microscope (JEOL).

4.2. Agarose fiber activation

CDAP activation of agarose and protein attachment was based on methods published by Kohn and Wilchek [40] with slight modifications: Agarose CNT ribbons were weighed (approximately 4 mg) and placed in a 20 mL glass scintillation vial (Fisher). The following solutions were added to vials each for (15 min) followed by aspiration and replacement with the next solution under gentle agitation. (1) Deionized water (10 mL) (twice), (2) 30% acetone (10 mL) (twice), (3) 60% acetone (10 mL) (twice). The last solution was then replaced with ice-cold 60% acetone (3 mL). Under agitation CDAP (Sigma) in dry acetonitrile (Sigma) (300 μL of 100 mg/mL) was added. After one min Et_3N (Sigma) (250 μL of 0.2 M) solution was added drop wise over one min. After five min of mixing, the solution from the vial was aspirated and transferred to a clean vial for activation verification. Ice cold (0.05 N) HCl (5 mL) was added to the fibers for five min mixing, followed by five min in cold deionized water (5 mL).

4.3 Protein Attachment

Functionalized fibers were added to either laminin (LN) (5mL of 20 ug/mL) from Engelbreth-Holm-Swarm murine sarcoma basement membrane (L2020, Invitrogen) or fluorescein conjugated bovine serum albumin (BSAC, A23015, Invitrogen) (5mL of 20 ug/mL) both in $NaHCO_3$ (0.1 M) for at least (16 h). Remaining active groups were quenched by adding of ethanolamine (Sigma) (150 μL) per 100 μL of attachment solution then stirring for 4 h. Fibers that underwent the full reaction were designated either “LN+” or “BSAC+”. Control fibers designated “LN−” or “BSA-” did not undergo the CDAP addition step but were added with the proteins. Another control group that was not added with any proteins and was designated “CDAP+”, while the pristine fibers were designated as such.

4.3.1. Washing—Fibers were washed for (15–20 min) in each of the following solutions: (1) deionized water (10 mL) (twice), (2) NaCl (10 mL, 0.5 M) (twice) (3) deionized water (10 mL) (twice). Fibers were then dried in nitrogen, sealed in airtight bags and refrigerated until use.

4.3.2. Activation verification—Qualitative verification of the activation of the agarose was performed as described by Kohn and Wilchek. [40] 1,3-dimethylbarbituric acid (Sigma) (0.15 g) was dissolved in pyridine (9 mL) and deionized water (1 mL). 2 mL of the resulting solution was added to the activation solution (100 μL).

4.3.3. Protein Attachment Verification—Visualization of the fibers using a fluorescent microscope can be performed. Fibers functionalized with BSAC, control fibers, and pristine fibers (those that did not undergo any reaction) were placed in either a clear or a black 96 well multi-well plate. The clear plate was placed within an inverted fluorescent microscope (Axio Observer-D1, Carl Zeiss MicroImaging GmbH) and imaged using a 10× objective. All fluorescent images were taken with similar exposure time to provide a true reflection of the intensity of the fluorescence. Fluorescent intensity recording from the black plate was taken using a well plate reader (M 200, Tecan). To allow background subtraction from the polypropylene, the fluorescence intensity of empty wells was measured and their average was subtracted from the readings of the fiber containing wells. The mean and standard deviations of fluorescent intensity (FI) measured using constant gains are presented in arbitrary units. To ensure laminin activation, 5 mm pieces of each type of fiber were placed in a 48 well plate (4 fibers per condition). Wells were added with phosphate buffer saline (PBS, Sigma Aldrich) (300 μL) containing 1% w/v of non-specific blocking serum (BSA, Sigma Aldrich) then gently shaken for 30 min. The solution was aspirated followed by 3 washes of the plates with PBS (500 μL each). A 1:100 dilution of rabbit polyclonal (300 μL) to laminin primary antibody (ab11575, Abcam) in PBS containing 1% BSA was added to each plate and incubated in room temperature overnight under gentle agitation. Wells were washed three times with PBS (500μL each), and a 1:50 dilution of secondary antibody (300 μL). Tetramethylrhodamine goat anti-rabbit IgG (T-2769, Invitrogen) was added to each well and incubated in room temperature for 4 h under gentle agitation followed by 5 washing steps and a final aspiration. The plate was kept in a dark and dry environment to allow evaporation of excess moisture. Fluorescent images and intensity reading of the fibers were taken as described for the BSAC functionalized fibers.

4.4. Conductivity Measurements

Fibers were partitioned into three batches based on whether either CDAP and / or LN were added to the reaction. Within each batch, three fibers were tested. Prior to testing, each end of the fiber was dipped in liquid nitrogen and clipped to expose a rigid cross section. Droplets of gallium/indium eutectic (liquid metal) was placed on each end of the fiber and the resistance was measured with a circuit-test DMR-5200 handheld multimeter. Eight measurements were taken and a statistical analysis was performed to compare the variance within each group and between groups. To test the fibers in buffer, the same procedure was used. However, in order to do so, a basin of vacuum grease was placed around the body of the fiber leaving the two fiber ends protruding out and untouched by the grease. Then the basin was filled with PBS. Resistance measurements were taken one h after filling the basin with PBS and 48 h after. This was repeated three times with batches of three different fibers.

4.5. Mechanical Testing

Tensile properties of the CNT fibers were tested using an MTS model Sintech 5/D tension machine, fitted with the (100 N) load cell at room temperature with 50% relative humidity. A minimum of 5 fibers per sample were tested. To evaluate the effect of the activation on the agarose, samples were hydrated by immersing individual fibers in PBS at (50 °C) (close to the agarose mp) under gentle agitation for one h. The mechanical testing was terminated when fibers reached their breakpoint. The mean and standard deviation of the secant modulus, yield stress and strain, and the maximal stress and strain are reported.

4.6. Cytotoxicity and Cell Attachment

Fibers were cut into 5mm pieces with a razorblade and placed into the wells of a Costar 96-well tissue-culture treated polystyrene plate. The plate was sterilized for 1 h in UV. Four types of fibers were used: CDAP+, LN−, LN+, and pristine fibers. Rat astrocytes, kindly

provided by John Frampton of the Wadsworth Center, were cultured in DMEM (Invitrogen), 10%FBS (Atlanta Biologicals), 1% Penicillin/Streptomycin at 37 °C, 5% CO_2. The cells were cultured to 90% confluence and then trypsinized, centrifuged, and the pellet re-suspended in media and the cells counted. 15,000 astrocytes were seeded into each well containing fiber and incubated for 18 h at (37 °C). 15,000 astrocytes were added to the positive and negative control wells. After 18 h, the media was aspirated from each well and washed with PBS. A 1:10 dilution of Alamar Blue (ABD Serotec) to regular media was prepared and 100ul of this mixture was added to each well. The cells were incubated for 5 h at (37 °C) and then a fluorescence measurement was recorded at 560 excitation and 590 emission using a Tecan Infinite M200 Fluorescent Plate Reader. The data obtained was normalized to the positive controls. To allow the evaluation of cell attachment on functionalized agarose CNT composites, dispersion films were prepared in the following manner: After sonication the CNT/agarose dispersion (90 μL) was sandwiched between two 12mm glass cover slips. Once cooled, flat gel capsule were formed. These capsules, with a composition similar to that of the fibers, underwent chemical modification in the same manner described for the fibers. Discs were places in a 24 well plate, sterilized under UV for 15 min, then washed with serum free culture media. Primary rat astrocytes (20 μl containing 100,000) were seeded onto the disks and incubated for two h to allow for cell attachment. Regular media was added to the wells containing the disks and the plates were incubated for three days. Afterward, the astrocyte-seeded disks were either (1) stained with Calcein AM (Invitrogen) followed by imaging using in the form of 3D data sets using a Leica SP2 confocal laser scanning inverted microscope with a 10× dry objective, or (2) fixed with 4% PFA for 15 min at (4°C). Following fixation, the cells were stained with 1:500 v/v Hoechst 33258 (Anaspec) and imaged using a Zeiss Axio Observer Fluorescent Microscope

4.7. *In Vivo* Characterization

4.7.1 Fiber Sterilization and Implantation—To allow accurate placement and smooth insertion of the fibers, a new insertion method developed in our lab was used. First a 24G × 3/4" catheter (Terumo, Somerset, NJ) was clipped. This allows the cannula and needle to be at the same length. The needle was withdrawn from the tip, and then the fiber was manually threaded into the now empty lumen tip. To insert the fibers into live tissue, the catheter was held above the insertion site using a mechanical arm, and a push of the needle drove the fiber into the required area without the needle penetrating the tissue. Prior to use, catheters with fibers were placed in self-sealing sterilizable pouches and sterilized with ethylene oxide gas (Anprolene; Anderson Products, Chapel Hill, NC) followed by 10 days aeration. Animal procedures were performed under the approval of the Wadsworth Center Institutional Animal Care and Use Committee (IACUC). Insertions were performed in a manner previously described with slight modifications[5]. Briefly, a (360 g) male Sprague–Dawley rat was anesthetized with 2.5% isoflurane with oxygen (1 l/min) for 5 min in a pre-exposed chamber, and then maintained with 2% isoflurane with oxygen for the duration of the procedure (60 min) in a stereotaxic holder. Four holes were drilled using electric drill (two on each side of midline, one anterior to bregma and one posterior to lambda). The dura was transected from the area of interest. Using a stereotactic holder, catheters were accurately placed above the insertion area, and a manual push of the needle allowed for smooth insertion of the fibers. Cellulose dialysis film (Fisher Scientific) was cut to 5 × 5 mm squares and applied over the exposed tissue, adhered to the scull and the skin was closed using staples.

4.7.2 Tissue Processing and Immunohistochemistry—14 days after implantation animal was sacrificed by first anesthetizing with a ketamine/xylazine mixture, followed by transcardial perfusion[62]. Tissue processing was performed based on standard immunohistochemistry (IHC) procedures[58]. Horizontal 80-μm-thick tissue slices were cut

using a vibratory microtome (Vibratom®, model 1000). Sections (900–1100 μm) down from the dorsal surface of the brain were used. Once sectioning was completed, fibers remaining in the intact tissue were gently removed and processed similarly to the brain slices. Histochemistry was performed on tissue slices and fibers labeling 3 cell types using the following reagents: Primary antibodies: (1) Astrocytes, rat anti-GFAP (Invitrogen, 13–0300, dilution 1:200) (2) Microglia, rabbit anti-Iba1 (019–19741, dilution 1:800, Wako, Richmond, VA. Secondary antibodies and added stain: (1) Goat anti-rabbit (Alexa Flour 488 A11008, dilution 1:200, Invitrogen) (2) Goat anti-rat (Alexa Flour 546 A110081, dilution 1:200, Invitrogen) (3) NeuroTrace stain for Nissl substance (530/615 N21482, Invitrogen). Sections were mounted on glass slides with ProLong Gold (Invitrogen) for confocal imaging. Histological images were collected in the form of 3D data sets using a Leica SP2 confocal laser scanning inverted microscope with a 10× dry objective. Images were stacked into X, Y projections of the entire Z dimension of the sample to allow for evaluation of cellular populations surrounding insertion sites. Images of the insertion site and two adjacent lateral fields were collected. Composite images were formed by aligning and superimposing through-focused projections of individual images using image-processing software (ImageJ, NIH). This allowed for observation of changes in immunohistochemistry immediately around the insertion sites and in control regions farther away. Fiber samples were imaged on both sides of the mounting slide since the black opaque nature of the fibers did not allow imaging of the full fiber thickness. One or two fields were collected for each side.

4.7.3 Image Quantification—Using ImageJ, individual channels were converted to 8 bit, followed by correction of the background and intensity. The radial profile plugin (by Paul Baggethun) was used to produces a profile plot of normalized integrated intensities around the implant site as a function of distance from the fiber center. The averaged intensity gradient maximized at the fibers edge is plotted along with the standard deviation in Figure 5.

Supplementary Material

Refer to Web version on PubMed Central for supplementary material.

Acknowledgments

This work was funded by National Institutes of Health under grant R01 EB007467-03, the Center for Neural Communication Technology (CNCT funded by the National Institutes of health under grant P41 EB000203) and the Graduate Assistance in Areas of National Need (GAANN) in pharmaceutical engineering. The content is solely the responsibility of the authors and does not necessarily represent the official views of the NIH, NIBIB,NCMHD or GAANN.

The authors would like to thank Anthony Ribaudo (TRI/Princeton) for expert guidance and assistance with SEM and Valery Starovoytov (Rutgers) for expert assistance with TEM.

References

1. Leach J, Achyuta AKH, Murthy SK. Frontiers in Neuroengineering. 2010; 3:12.
2. Ryu SI, Shenoy KV. Neurosurgical Focus. 2009; 27
3. Polikov VS, Tresco PA, Reichert WM. J Neurosci Methods. 2005; 148:1. [PubMed: 16198003]
4. Shain W, Spataro L, Dilgen J, Haverstick K, Retterer S, Isaacson M, Saltzman M, Turner JN. Controlling cellular reactive responses around neural prosthetic devices using peripheral and local intervention strategies. 2003.
5. Szarowski DH, Andersen MD, Retterer S, Spence AJ, Isaacson M, Craighead HG, Turner JN, Shain W. Brain Res. 2003; 983:23. [PubMed: 12914963]
6. Zhong YH, Bellamkonda RV. Brain Res. 2007; 1148:15. [PubMed: 17376408]

7. Abidian MR, Martin DC. Advanced Functional Materials. 2009; 19:573.
8. Mercanzini A, Reddy ST, Velluto D, Colin P, Maillard A, Bensadoun J-C, Hubbell JA, Renaud P. Journal of Controlled Release. 2010; 145:196. [PubMed: 20447428]
9. Marin C, Fernandez E. Front Neuroengineering. 2010; 3:8.
10. Purcell EK, Thompson DE, Ludwig KA, Kipke DR. Journal of Neuroscience Methods. 2009; 183:149. [PubMed: 19560490]
11. He W, McConnell GC, Schneider TM, Bellamkonda RV. Advanced Materials. 2007; 19:3529.
12. Azemi E, Stauffer WR, Gostock MS, Lagenaur CF, Cui XT. Acta Biomaterialia. 2008; 4:1208. [PubMed: 18420473]
13. Winslow BD, Christensen MB, Yang W-K, Solzbacher F, Tresco PA. Biomaterials. 2010; 31:9163. [PubMed: 20561678]
14. Chen C-H, Chuang S-C, Lee Y-T, Chang Y-C, Yeh S-R, Yao D-J. Journal of Micro/Nanolithography, MEMS and MOEMS. 2010; 9:031007.
15. Kozai TDY, Kipke DR. Journal of Neuroscience Methods. 2009; 184:199. [PubMed: 19666051]
16. Foley CP, Nishimura N, Neeves KB, Schaffer CB, Olbricht WL. Biomedical Microdevices. 2009; 11:915. [PubMed: 19353271]
17. Seymour JP, Kipke DR. Biomaterials. 2007; 28:3594. [PubMed: 17517431]
18. Jaroch DB, Ward MP, Chow EY, Rickus JL, Irazoqui PP. Journal of Neuroscience Methods. 2009; 183:213. [PubMed: 19596378]
19. Kipke DR, Shain W, Buzsaki G, Fetz E, Henderson JM, Hetke JF, Schalk G. J. Neurosci. 2008; 28:11830. [PubMed: 19005048]
20. Freeman MR. Science. 2010; 330:774. [PubMed: 21051628]
21. Dalton AB, Collins S, Munoz E, Razal JM, Ebron VH, Ferraris JP, Coleman JN, Kim BG, Baughman RH. Nature. 2003; 423:703. [PubMed: 12802323]
22. Neimark AV, Ruetsch S, Kornev KG, Ravikovitch PI. Nano Lett. 2003; 3:419.
23. Vigolo B, Penicaud A, Coulon C, Sauder C, Pailler R, Journet C, Bernier P, Poulin P. Science. 2000; 290:1331. [PubMed: 11082056]
24. Dubin RA, Callegari GC, Kohn J, Neimark AV. IEEE Trans. Nanobiosci. 2008; 7:11.
25. Jan E, Kotov NA. Nano Lett. 2007; 7:1123. [PubMed: 17451277]
26. Chao TI, Xiang SH, Chen CS, Chin WC, Nelson AJ, Wang CC, Lu J. Biochem. Biophys. Res. Commun. 2009; 384:426. [PubMed: 19426708]
27. Tay CY, Gu HG, Leong WS, Yu HY, Li HQ, Heng BC, Tantang H, Loo SCJ, Li LJ, Tan LP. Carbon. 48:1095.
28. Granero AJ, Razal JM, Wallace GG, Panhuis MIH. Adv. Funct. Mater. 2008; 18:3759.
29. Lynam C, Moulton SE, Wallace GG. Adv. Mater. 2007; 19:1244.
30. Neri W, Maugey M, Miaudet P, Derre A, Zakri C, Poulin P. Macromol. Rapid Commun. 2006; 27:1035.
31. Razal JM, Gilmore KJ, Wallace GG. Adv. Funct. Mater. 2008; 18:61.
32. Spinks GA, Shin SR, Wallace GG, Whitten PG, Kim IY, Kim SI, Kim SJ. Sens. Actuator B-Chem. 2007; 121:616.
33. Thompson BC, Moulton SE, Gilmore KJ, Higgins MJ, Whitten PG, Wallace GG. Carbon. 2009; 47:1282.
34. Xu XZ, Uddin AJ, Aoki K, Gotoh Y, Saito T, Yumura M. Carbon. 2010; 48:1977.
35. Hynd MR, Frampton JP, Dowell-Mesfin N, Turner JN, Shain W. J. Neurosci. Methods. 2007; 162:255. [PubMed: 17368788]
36. Rago AP, Napolitano AP, Dean DM, Chai PR, Morgan JR. Cytotechnology. 2008; 56:81. [PubMed: 19002845]
37. Nisbet DR, Crompton KE, Horne MK, Finkelstein DI, Forsythe JS. Journal of Biomedical Materials Research Part B: Applied Biomaterials. 2008; 87B:251.
38. Luo Y, Shoichet MS. Nat Mater. 2004; 3:249. [PubMed: 15034559]
39. Yu XJ, Dillon GP, Bellamkonda RV. Tissue Engineering. 1999; 5:291. [PubMed: 10477852]

40. Kohn J, Wilchek M. Applied Biochemistry and Biotechnology. 1984; 9:285.
41. Pernodet N, Maaloum M, Tinland B. Electrophoresis. 1997; 18:55. [PubMed: 9059821]
42. Gros T, Sakamoto JS, Blesch A, Havton LA, Tuszynski MH. Biomaterials. 2010; 31:6719. [PubMed: 20619785]
43. Kornev KG, Callegari G, Kuppler J, Ruetsch S, Neimark AV. Phys. Rev. Lett. 2006; 97:4.
44. Cellot G, Cilia E, Cipollone S, Rancic V, Sucapane A, Giordani S, Gambazzi L, Markram H, Grandolfo M, Scaini D, Gelain F, Casalis L, Prato M, Giugliano M, Ballerini L. Nat. Nanotechnol. 2009; 4:126. [PubMed: 19197316]
45. Blighe FM, Young K, Vilatela JJ, Windle AH, Kinloch IA, Deng L, Young RJ, Coleman JN. Adv. Funct. Mater. 21:364.
46. Sharp AA, Ortega AM, Restrepo D, Curran-Everett D, Gall K. Biomedical Engineering, IEEE Transactions on. 2009; 56:45.
47. Hrapko M, van Dommelen JA, Peters GW, Wismans JS. Biorheology. 2008; 45:663. [PubMed: 19065013]
48. Shafer DE, Toll B, Schuman RF, Nelson BL, Mond JJ, Lees A. Vaccine. 2000; 18:1273. [PubMed: 10649629]
49. Normand V, Lootens DL, Amici E, Plucknett KP, Aymard P. Biomacromolecules. 2000; 1:730. [PubMed: 11710204]
50. Jones DG, Anderson ER, Galvin KA. Neurorehabilitation. 2003; 18:339. [PubMed: 14757930]
51. Gheith MK, Sinani VA, Wicksted JP, Matts RL, Kotov NA. Adv. Mater. 2005; 17:2663.
52. Hu H, Ni YC, Montana V, Haddon RC, Parpura V. Nano Lett. 2004; 4:507. [PubMed: 21394241]
53. Lovat V, Pantarotto D, Lagostena L, Cacciari B, Grandolfo M, Righi M, Spalluto G, Prato M, Ballerini L. Nano Lett. 2005; 5:1107. [PubMed: 15943451]
54. Galano A. Nanoscale. 2010; 2:373. [PubMed: 20644818]
55. HajjHassan M, Chodavarapu V, Musallam S. Sensors. 2008; 8:6704.
56. Shvedova AA, Castranova V, Kisin ER, Schwegler-Berry D, Murray AR, Gandelsman VZ, Maynard A, Baron P. J. Toxicol. Env. Health Pt A. 2003; 66:1909.
57. Shvedova AA, Kisin ER, Mercer R, Murray AR, Johnson VJ, Potapovich AI, Tyurina YY, Gorelik O, Arepalli S, Schwegler-Berry D, Hubbs AF, Antonini J, Evans DE, Ku BK, Ramsey D, Maynard A, Kagan VE, Castranova V, Baron P. Am. J. Physiol.-Lung Cell. Mol. Physiol. 2005; 289:L698. [PubMed: 15951334]
58. Szarowski DH, Andersen MD, Retterer S, Spence AJ, Isaacson M, Craighead HG, Turner JN, Shain W. Brain Res. 2003; 983:23. [PubMed: 12914963]
59. Grill WM, Norman SE, Bellamkonda RV. Annu. Rev. Biomed. Eng. 2009; 11:1. [PubMed: 19400710]
60. Webb K, Budko E, Neuberger TJ, Chen SZ, Schachner M, Tresco PA. Biomaterials. 2001; 22:1017. [PubMed: 11352083]
61. Ruiter GCW, Malessy MJA, Yaszemski MJ, Windebank AJ, Spinner RJ. Neurosurg. Focus. 2009; 26:9.
62. Bjornsson CS, Lin G, Al-Kofahi Y, Narayanaswamy A, Smith KL, Shain W, Roysam B. J. Neurosci. Methods. 2008; 170:165. [PubMed: 18294697]

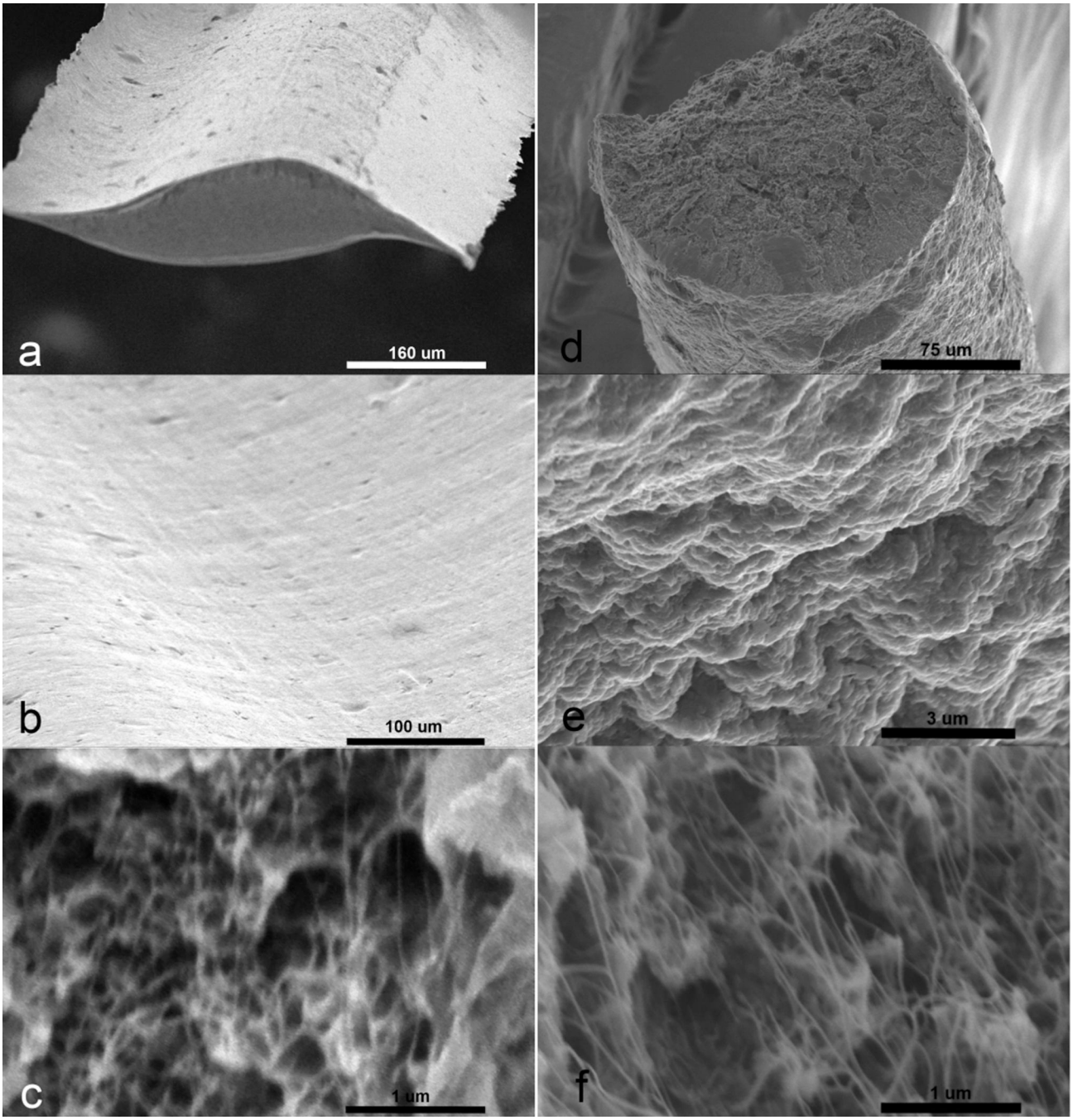

Figure 1.
Scanning Electron Microscopy images of CNT agarose fibers. Left, molded fibers a) cross section of the fiber, b) close up of the fiber body depicting the smooth morphology of the surface, c) Close up of the cross section depicting the carbon nanotube bundles. Right, wet spun agarose fibers d) cross section of the fiber, e) close up of the fiber body depicting the rough morphology f) close up of the cross section depicting the carbon nanotube bundles.

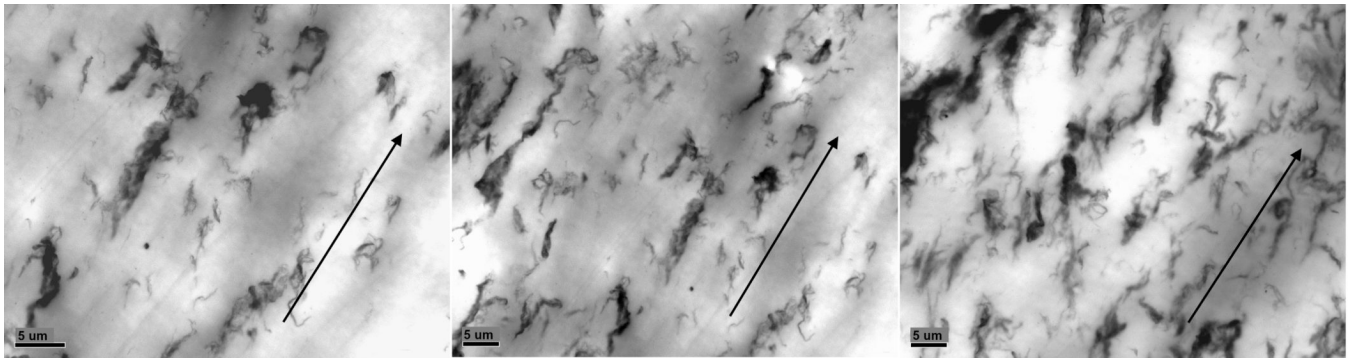

Figure 2.
TEM images of molded fibers demonstrating fiber orientation in the direction of molding indicated by the arrows.

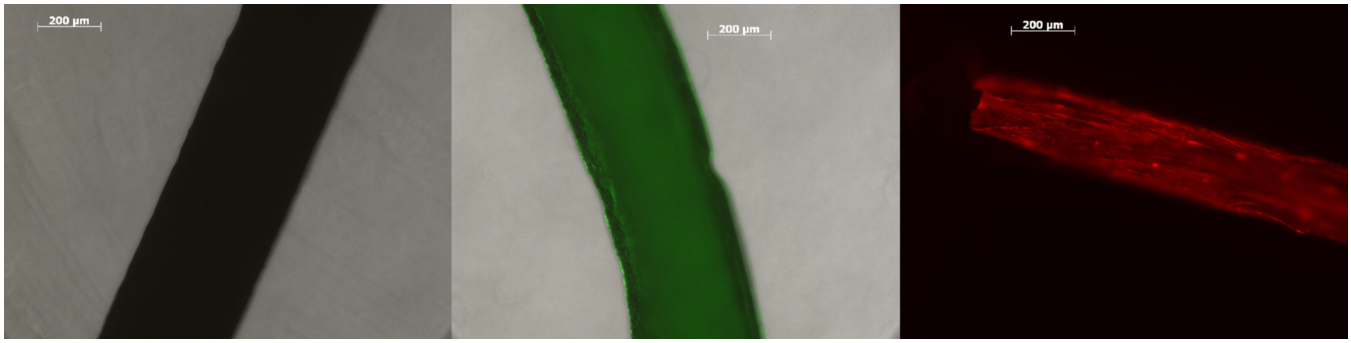

Figure 3.

(A) Merged fluorescent and phase contrast image of BSAC− conjugate control fiber (B) Merged fluorescent and phase contrast image of BSAC+ conjugate functionalized fiber. (C) Fluorescent image LN+ Laminin functionalized fiber. The exposure time to the fluorescent channels were kept constant to eliminate gain variability and false images. Fluorescent intensity (FI) reading from fibers placed in a well plate then scanned through a plate reader. D) LN reactions. E) BSAC reactions. Samples designation: CDAP+ are controls without protein added. LN+ and BSAC+ are protein functionalized. LN− and BSAC− are controls without protein added.

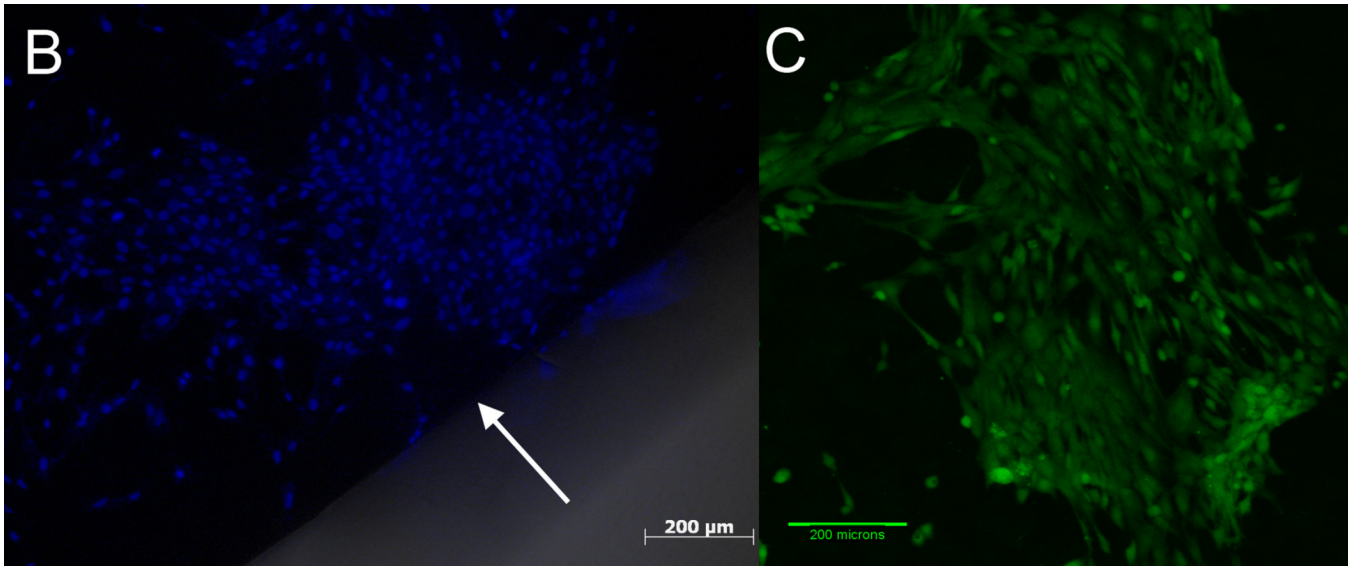

Figure 4.

A) Cell viability after 24 h exposure to four types of fibers. Data is plotted against positive control. B) Projected phase contrast and fluorescent images of DAPI stained fixed astrocytes grown on LN+ disc after 3 d incubation. Edge of disc is marked by white arrows. Cells are solidly attached to only the agar disc. C) Projected confocal image of live astrocytes grown on LN+ stained with Calcein AM after 3 d incubation. Scale bars are (200 µm)

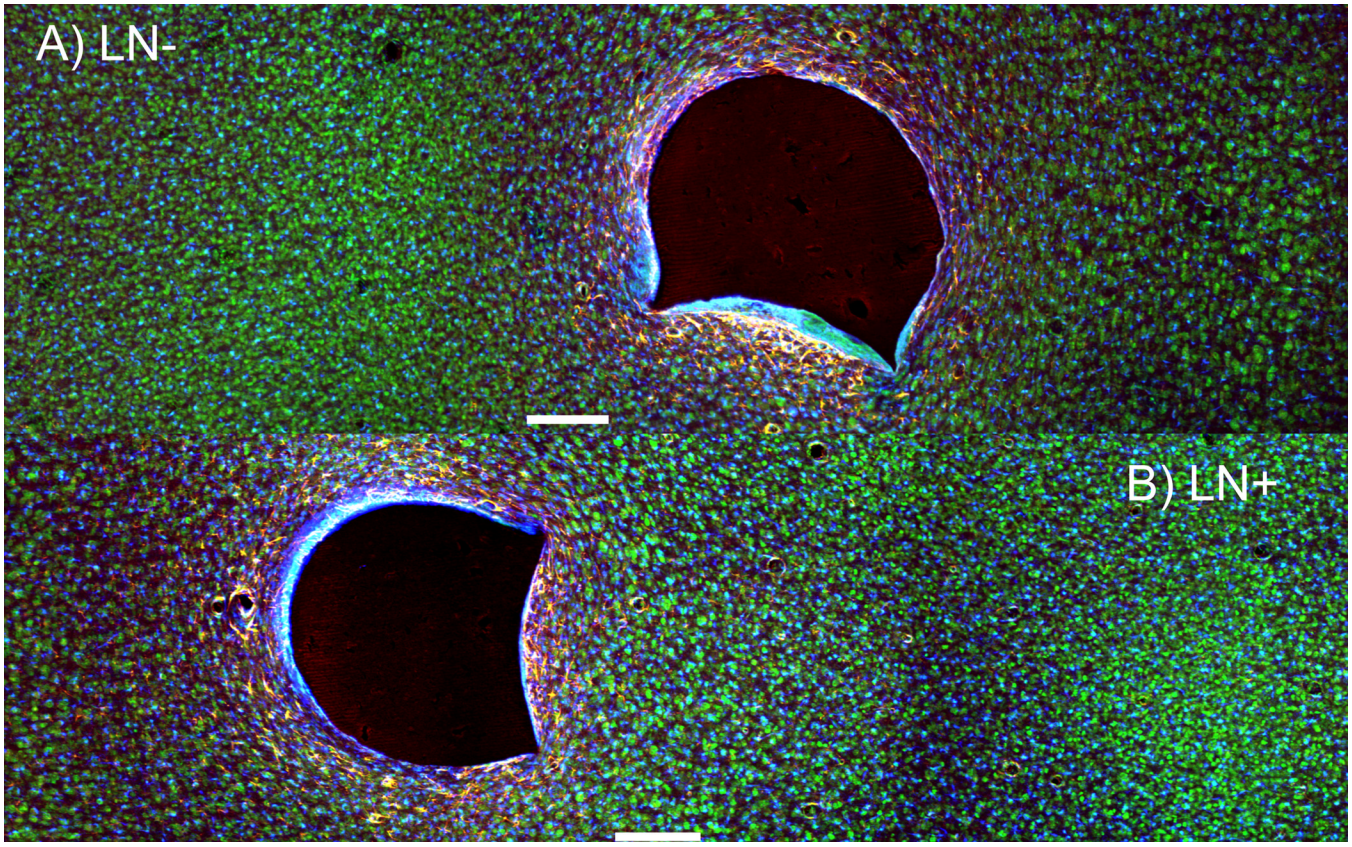

Figure 5.
Representative immunohistochemical images of fibers inserted into rat cortex. A) LN− fiber, B) LN+ fiber, yellow – astrocytes (GFAP). blue – microglia (Iba-1). green - neurons (Nissl). Scale bar 100 μm. Favorable tissue reaction to the laminin tethered fiber can be observed by quantifying the normalized individual cellular response to the implants, where reduced microglia and astrocyte response (C & D respectively), with increased neural expression (D) can be seen.

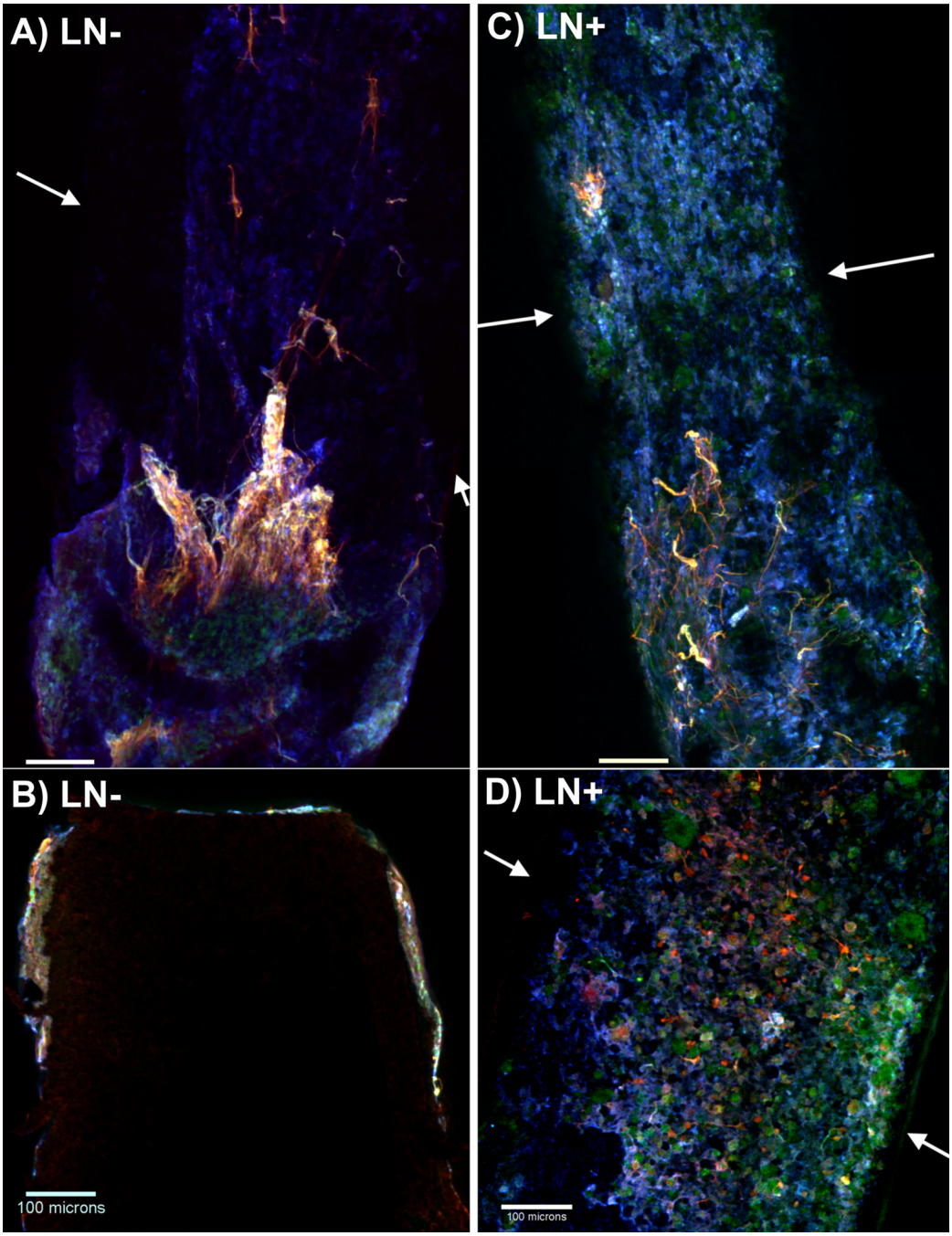

Figure 6.

Projection confocal images of fibers extracted from brains. Images are of two sides of each fiber mounted on the glass slide (designated as LN− and LN+). Yellow – astrocytes (GFAP). Blue – microglia (Iba-1). Green – Neurons (Nissl). The micrograph of the laminin functionalized fiber (LN+, C and D) demonstrates a greater attachment of all cell types when compared to non-functionalized (LN−, A and B) fiber. Non-specific cell attachment is more evident with the LN+ fibers. Scale bar 100 μm)

Table 1

Tensile results for different agarose/SWNT fibers in dry and hydrated states.

Sample		Modulus [MPa]	Yield Stress [MPa]	Yield Strain [%]	Max Strain [%]
Pristine	Dry	1280 ± 386	17.3 ± 5.1	1.8 ± 0.8	8.3 + 2.0
	Hydrated	0	0	0	0
LN+	Dry	867 ± 247	14.3 ± 4.8	1.9 ± 0.7	6.2 ± 2.5
	Hydrated	85.6 ± 12.8	0.1 ± 0	4.7 ± 2	4.8 ± 1.8
CDAP+	Dry	1060 ± 698	5.2 ± 0.6	0.7 ± 0.5	8.9 ± 0.3
	Hydrated	220 ± 120	0.6 ± 0	4.2 ± 2.8	10.5 ± 4.2

Table 2

Specific conductivities of fibers in the dry state, and 1 and 48 h after wetting. Conductivity retention in % is indicated as well.

	Specific Conductivity [S cm^{-1}]				
Fiber type	**Dry**	**1 h wet**	**Retention**	**48 h wet**	**retention**
Pristine	191 ± 14	6 ± 1	3 %	3 ± 0	2 %
LN+	145 ± 0	64 ± 4	44 %	67 ± 1	46 %
CDAP+	131 ± 1	131 ± 4	100 %	135 ± 55	103 %